Monthly Notices
of the
ROYAL ASTRONOMICAL SOCIETY

MNRAS **466,** L1–L6 (2017)
Advance Access publication 2016 October 13

doi:10.1093/mnrasl/slw210

# NIHAO – XI. Formation of ultra-diffuse galaxies by outflows

Arianna Di Cintio,[1⋆] Chris B. Brook,[2] Aaron A. Dutton,[3] Andrea V. Macciò,[3,4] Aura Obreja[3] and Avishai Dekel[5]

[1]*Dark Cosmology Centre, NBI, University of Copenhagen, Juliane Maries Vej 30, DK-2100 Copenhagen, Denmark*
[2]*Instituto de Astrofísica de Canarias, Universidad de La Laguna, E-38206 La Laguna, Tenerife, Spain*
[3]*New York University Abu Dhabi, PO Box 129188 Abu Dhabi, UAE*
[4]*Max Planck Institute für Astronomie, Königstuhl 17, D-69117 Heidelberg, Germany*
[5]*Center for Astrophysics and Planetary Science, Racah Institute of Physics, The Hebrew University, Jerusalem 91904, Israel*

Accepted 2016 October 11. Received 2016 October 10; in original form 2016 August 3

## ABSTRACT

We address the origin of ultra-diffuse galaxies (UDGs), which have stellar masses typical of dwarf galaxies but effective radii of Milky Way-sized objects. Their formation mechanism, and whether they are failed $L_\star$ galaxies or diffuse dwarfs, are challenging issues. Using zoom-in cosmological simulations from the Numerical Investigation of a Hundred Astrophysical Objects (NIHAO) project, we show that UDG analogues form naturally in dwarf-sized haloes due to episodes of gas outflows associated with star formation. The simulated UDGs live in isolated haloes of masses $10^{10–11}$ $M_\odot$, have stellar masses of $10^{7–8.5}$ $M_\odot$, effective radii larger than 1 kpc and dark matter cores. They show a broad range of colours, an average Sérsic index of 0.83, a typical distribution of halo spin and concentration, and a non-negligible H I gas mass of $10^{7-9}$ $M_\odot$, which correlates with the extent of the galaxy. Gas availability is crucial to the internal processes which form UDGs: feedback-driven gas outflows, and subsequent dark matter and stellar expansion, are the key to reproduce faint, yet unusually extended, galaxies. This scenario implies that UDGs represent a dwarf population of low surface brightness galaxies and should exist in the field. The largest isolated UDGs should contain more H I gas than less extended dwarfs of similar $M^\star$.

**Key words:** galaxies: dwarf – galaxies: evolution – galaxies: formation – galaxies: haloes.

## 1 INTRODUCTION

Deep imaging of nearby clusters have revealed a sizeable population of faint, $M_R \gtrsim -16.5$, low surface brightness (LSB), $\mu_e =$ 24–28 mag arcsec$^{-2}$, and unusually large, $0.8 < r_e/\mathrm{kpc} < 5$ galaxies, named ultra-diffuse galaxies or UDGs (van Dokkum et al. 2015a). While their stellar masses are typical of dwarfs, $10^7 < M^\star/M_\odot < 10^{8.7}$, their effective radii are compatible with $L_\star$ objects, raising doubts about the nature of such galaxies. Almost 1000 UDGs have been identified in the Coma cluster using the Dragonfly array (van Dokkum et al. 2015a,b) and the Subaru telescope (Koda et al. 2015; Yagi et al. 2016): they represent a passively evolving population, lying on the red sequence in the colour–magnitude diagram, as opposed to classical LSB galaxies, which are bluer and brighter (e.g. McGaugh, Schombert & Bothun 1995; Impey & Bothun 1997; Schombert, Maciel & McGaugh 2011). Red UDGs have since been found in the Virgo cluster (Mihos et al. 2015), with even lower SB than the Virgo LSBs discovered 30 years ago by Sandage & Binggeli (1984). Confirming the existence of an abundant population of such objects, UDGs have also been observed in Fornax and other clusters (Muñoz et al. 2015; van der Burg, Muzzin & Hoekstra 2016). However, UDGs may not necessarily be red and associated with clusters: Roman & Trujillo (2016) studied a region around the Abell 168 cluster, showing that about half of its UDGs are found outside the main cluster overdensity, with their properties changing towards the cluster centre, suggestive of environmental effects; they also observed bluer UDGs than in Coma. Corroborating the idea that UDGs can form in isolation, Martínez-Delgado et al. (2016) found a UDG in the outskirts of the Pisces–Perseus supercluster, DGSAT I, which shows a blue overdensity compatible with recent star formation.

While some authors envision a scenario in which UDGs are failed $L_\star$ galaxies which lost their gas after forming the first stars (van Dokkum et al. 2015a,b), some others argue that they are genuine dwarf galaxies possibly living in high-spin haloes (Amorisco & Loeb 2016). Supporting the first claim are simulations by Yozin & Bekki (2015), indicating that UDGs may be underdeveloped galaxies whose early accretion on to a cluster quenched further growth. Favouring a massive halo for UDGs is the inferred virial mass of $\sim 8 \times 10^{11}$ $M_\odot$ for DF 44,[1] one of the brightest Coma UDGs

[1] The Macciò, Dutton & van den Bosch (2008) *c–M* relation was used, giving up to 30 per cent lower concentration than the *Planck* one used here, allowing a fit into a larger halo.

⋆ E-mail: arianna.dicintio@dark-cosmology.dk

(van Dokkum et al. 2016). This result is in contrast with the derived mass of two other UDGs: using the abundance of their globular clusters, Beasley et al. (2016) inferred a $M_{\rm halo}$ of $(8 \pm 4) \times 10^{10}$ $M_\odot$ for VCC 1287, while Peng & Lim (2016) and Beasley & Trujillo (2016) determined a total mass of $(\sim 9 \pm 2) \times 10^{10}$ $M_\odot$ for DF17, favouring the idea that UDGs are dwarfs. Further, Roman & Trujillo (2016) showed that the spatial distribution of UDGs in Abell 168 is compatible with the one of standard dwarfs.

A key question is whether UDGs can arise within a $\lambda$ cold dark matter universe. An appealing possibility is that the formation of UDGs is not connected to the cluster environment, but rather to internal processes, such that UDGs already have a spatially extended stellar component when infalling into a cluster. Previous simulation works extensively showed that feedback-driven gas outflows are able to cause expansion not only of the central dark matter (DM) distribution in galaxies (e.g. Governato et al. 2010; Di Cintio et al. 2014a,b; Chan et al. 2015; Oñorbe et al. 2015; Read, Agertz & Collins 2016; Tollet et al. 2016), but also of the stellar one (e.g. Teyssier et al. 2013; Dutton et al. 2016; El-Badry et al. 2016). The formation of DM density cores is related to rapid oscillation of the central potential driven by gas outflows following bursty star formation (e.g. Read & Gilmore 2005; Mashchenko, Wadsley & Couchman 2008; Pontzen & Governato 2012) and has been applied to observations to reconcile the *cusp-core* discrepancy (Katz et al. 2016). Interestingly, the mass range where we expect maximum efficiency in core formation overlaps with that of UDGs, i.e. galaxies with $M^\star \sim 10^{7-9}$ $M_\odot$ should form large DM and stellar cores, while at higher and lower masses energy from stellar feedback alone becomes less efficient at creating cores (Di Cintio et al. 2014a,b; Dutton et al. 2016). It is thus natural to explore whether feedback-driven expansion is a viable mechanism for the formation of UDGs. In this Letter, we show that isolated UDGs, with a spatially extended stellar distribution, form naturally in dwarf-sized haloes by gas outflows. In Section 2, we introduce the hydrodynamical cosmological simulations used; in Section 3, we investigate the formation scenario of UDGs and show results focusing on global properties and gas content of UDGs; and in Section 4, we conclude by highlighting some observational predictions of our model.

## 2 SIMULATIONS

The simulated galaxies are taken from the Numerical Investigation of a Hundred Astrophysical Objects (NIHAO) project (Wang et al. 2015), evolved using the SPH code Gasoline (Wadsley, Stadel & Quinn 2004; Keller et al. 2014). The code includes a subgrid model for turbulent mixing of metals and energy (Wadsley, Veeravalli & Couchman 2008), ultraviolet heating, ionization and metal cooling (Shen, Wadsley & Stinson 2010). Star formation and feedback follows the model used in the MaGICC simulations (Stinson et al. 2013), which for the first time reproduced several galaxy scaling relations over a wide mass range (Brook et al. 2012), adopting a threshold for star formation of $n_{\rm th} > 10.3$ cm$^{-3}$.

Stars feed energy back into the interstellar medium via blast-wave supernova feedback (Stinson et al. 2006) and early stellar feedback from massive stars. Particle masses and force softenings are chosen to resolve the mass profile to below 1 per cent of the virial radius at all masses, ensuring that galaxy half-light radii are well resolved. The NIHAO galaxies cover a broad mass range, from dwarfs to Milky Way mass, and represent an unbiased sampling of merger histories, concentrations and spin parameters. The galaxies are all centrals and isolated, and lie on abundance matching predictions, having the expected $M^\star$ for each $M_{\rm halo}$. The NIHAO project satisfactorily reproduces realistic galaxies in terms of their $M^\star$, SFH, metals and DM distribution (e.g. Obreja et al. 2016; Tollet et al. 2016). The haloes are identified using the AHF halo finder (Knollmann & Knebe 2009) and partially analysed with the PYNBODY package (Pontzen et al. 2013).

## 3 RESULTS

Simulated galaxies are defined as UDGs if they satisfy the following criteria: (i) their 2D effective radius, $r_{\rm e}$, is larger than 1 kpc, (ii) their absolute magnitude in $R$-band is $-16.5 \lesssim M_{\rm R} \lesssim -12$, corresponding to a stellar mass of $10^7 \lesssim M^\star/{\rm M}_\odot \lesssim 10^{8.5}$, (iii) their effective surface brightness is low, with $\mu_{\rm e} > 23.5$ mag arcsec$^{-2}$. It is worth noticing that several of the NIHAO galaxies fall in the UDGs category. To facilitate comparisons with observational results, we work in the AB system and used $UBVR_{\rm c}I_{\rm c}$ Johnson–Cousins filters. Galaxies are face-on (aligned via angular momentum of the stars) when computing $r_{\rm e}$ and the effective surface brightness is defined as $L/(2\pi r_{\rm e}^2)$ before converting it in units of mag arcsec$^{-2}$.

A sample of 21 NIHAO simulations meets these requirements, shown in Fig. 1 as black points, with the largest sized UDGs ($r_{\rm e} \geq 2$ kpc) further circled. One of the most extreme UDGs, with the largest $r_{\rm e}$ amongst the lowest surface brightness objects, is marked with a cross in Fig. 1 and it will be analysed in Section 3.2. In Fig. 1, we compare simulations with observed UDGs. From top to bottom, the colour $B-R$, the 2D effective radius and the effective surface brightness are shown against the absolute magnitude $M_{\rm R}$. SDSS *gri* colours and magnitudes used in Roman & Trujillo (2016) were converted to $B-R$ Subaru–Suprime–Cam ones used in Yagi et al. (2016) by adopting the colour conversions derived in the appendix of Yoshida et al. (2016). When comparing $r_{\rm e}$ and $\mu_{\rm e}$ with the Roman & Trujillo (2016) data we used their $R$-band results, as best approximation of our $R$-band ones.

Simulated UDGs overlap with observational data in colour, effective radii, surface brightness and magnitude. While most of the Coma cluster UDGs follow the red sequence with $B-R = 0.8$–$1.2$, the Abell 168 region, including both cluster and field UDGs, span a wider range in colours, with the bluest objects having $B-R \sim 0.4$. This broad range in colours is also observed in the simulated UDGs, some of which have recent star formation (see Section 3.3), an indication that not all UDGs are evolving passively and suggesting that the isolated counterparts of cluster UDGs may not be quenched.

### 3.1 UDGs: global properties of the simulated sample

In Table 1, we summarize the properties of simulated UDGs: from top to bottom, we specify stellar mass, halo mass, H I gas mass ($M_{\rm H\,I}$), 2D effective radius, effective surface brightness, $R$-band absolute magnitude, $B-R$ colour, Sérsic index, DM halo inner slope, spin parameter and concentration. Specifically, the Sérsic index $n_{\rm Sersic}$ is computed by fitting the 2D surface brightness profile in $R$ band out to $2 \times r_{\rm e}$ with a Sérsic profile (Sersic 1968), the inner slope $\gamma$ of the DM halo is found by fitting its density profile with a power law between 1 and 2 per cent of the virial radius, in a region where all our galaxies are well resolved, the dimensionless spin parameter $\lambda$ follows the Bullock et al. (2001) definition and the concentration $c$ is computed from the original DM-only simulation.

All the currently observed structural properties of UDGs ($M^\star$, $n_{\rm Sersic}$, colour, $M_{\rm R}$, $r_{\rm e}$ and $\mu_{\rm e}$) are in excellent agreement with the ones of the simulated sample. The mean value of the spin parameter is close to the peak of the distribution of spin parameters for DM haloes [$\log(\lambda \sim -1.45)$, Bullock et al. 2001, indicating that our

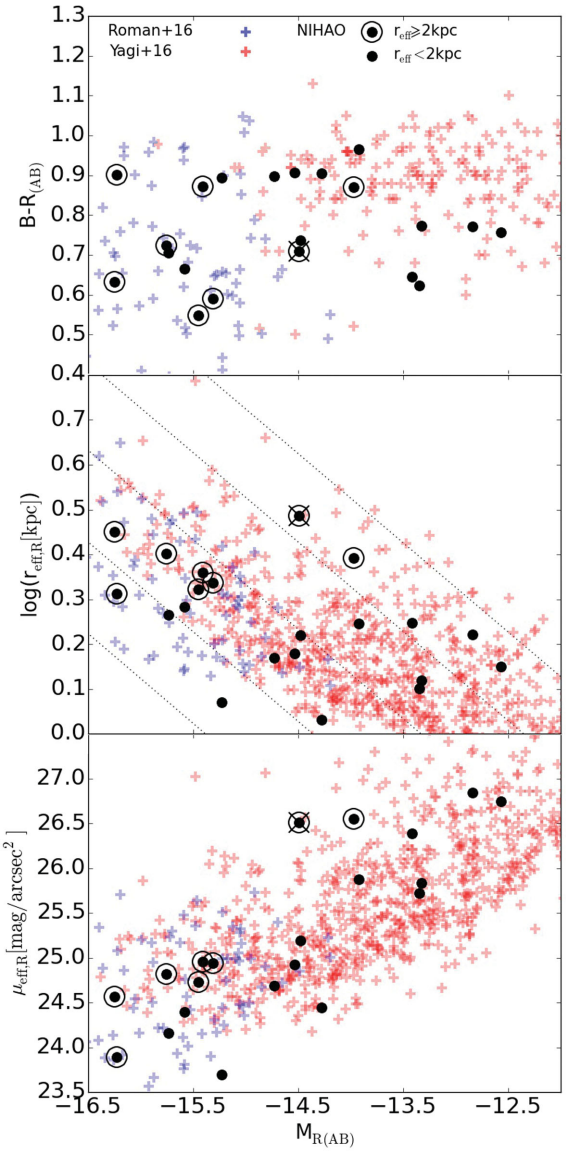


**Figure 1.** From top to bottom, we show B–R, $r_e$ and $\mu_e$ as a function of $R$-band absolute magnitude of Coma cluster UDGs from Yagi et al. (2016) (red crosses) and of Abell 168 cluster and field UDGs from Roman & Trujillo (2016) (blue crosses). Diagonal lines represent constant $\mu_e$ lines. Simulated UDGs with effective radii $1 < r_e/\mathrm{kpc} < 2$ are shown as black points, with extreme cases, $r_e \geq 2$ kpc, further circled. The crossed UDG is analysed in Section 3.2 and Fig. 3.

**Table 1.** Average properties of the simulated UDG sample. Concentrations and spin parameters have been computed in the original DM-only run.

| $X$ | $\overline{X} \pm \sigma$ | $X_{\mathrm{min,max}}$ |
|---|---|---|
| $\log[M^\star(\mathrm{M}_\odot)]$ | 7.66 ± 0.42 | 6.83, 8.40 |
| $\log[M_{\mathrm{halo}}(\mathrm{M}_\odot)]$ | 10.53 ± 0.18 | 10.22, 10.85 |
| $\log\{M_{\mathrm{H\,I}}(\mathrm{M}_\odot)\}$ | 8.37 ± 0.59 | 7.22, 9.24 |
| $r_e$ (kpc) | 1.87 ± 0.53 | 1.07, 3.06 |
| $\mu_e$(mag arcsec$^{-2}$) | 25.23 ± 0.94 | 23.69, 26.84 |
| $M_R$ | −14.61 ± 1.07 | −16.25, −12.57 |
| $B-R$ | 0.77 ± 0.12 | 0.54, 0.97 |
| $n_{\mathrm{Sersic}}$ | 0.83 ± 0.27 | 0.31, 1.46 |
| $\gamma$(1–2 per cent $R_{\mathrm{vir}}$) | −0.37 ± 0.18 | −0.78, −0.01 |
| $\log(\lambda)$ | −1.48 ± 0.25 | −2.04, −1.17 |
| $c_{\mathrm{DM}}$ | 10.67 ± 3.05 | 5.89, 18.85 |

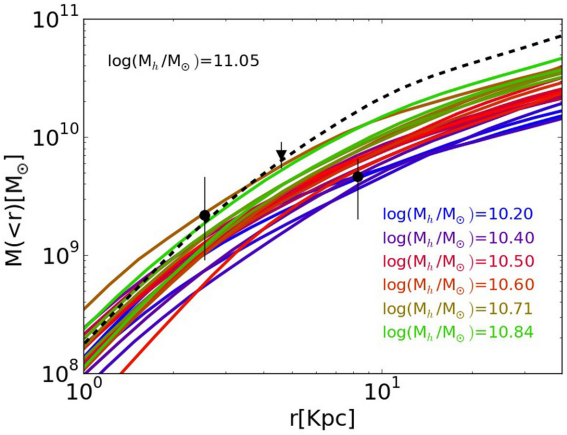


**Figure 2.** Mass profiles of simulated UDGs, colour coded by DM halo mass, including contributions from DM, gas and stars. Overplotted observational results from Beasley et al. (2016), VCC 1287 UDG as circles points, and from van Dokkum et al. (2016), DF 44 UDG as triangle.

simulated UDGs do not live in particularly high-spin objects as suggested by Amorisco & Loeb (2016). The range of DM inner slopes, $-0.78 < \gamma < -0.01$, shows that UDGs live in expanded DM haloes, whose logarithmic inner slope is shallower than the universal NFW value of $\gamma = -1$. We will see in Section 3.2 how this is closely linked to the formation of UDGs.

Interestingly, the simulated UDGs have a non-negligible amount of H I gas, whose fraction at $z = 0$ is computed including self-shielding and ionization from star-forming regions as in Gutcke et al. (2016). While most recent observations focused on UDGs in clusters, finding the not surprising result that those objects are gas poor, there is no current evidence that isolated UDGs should be gas poor: indeed, the only work which focused on isolated UDGs could only place an upper limit of $M_{\mathrm{H\,I}} < 10^{8.8}$ M$_\odot$ on the expected amount of H I gas in DGSAT I (Martínez-Delgado et al. 2016), suggesting that values of $7 \lesssim \log_{10}(M_{\mathrm{H\,I}}/\mathrm{M}_\odot) \lesssim 9$, as predicted by our simulations, are fully within observational constraints. Note that the $M_{\mathrm{H\,I}}$ amount which UDGs should have once falling into a cluster cannot be inferred by using our isolated simulations. Remarkably, the simulated UDGs have average halo mass $M_{\mathrm{halo}} = 10^{10.53}$ M$_\odot$ and a maximum and minimum $M_{\mathrm{halo}}$ of $10^{10.22}$ and $10^{10.85}$ M$_\odot$, respectively: they are therefore legitimate dwarfs rather than failed $L\star$ objects. Such dwarf halo mass range is also advocated in Amorisco & Loeb (2016), although their model requires high halo spin, unlike what we see in our simulated UDGs.

The halo masses of the simulated galaxies are in agreement with the inferred mass of UDGs in the Virgo (Beasley et al. 2016) and Coma clusters (Beasley & Trujillo 2016; Peng & Lim 2016). We plot in Fig. 2 their total mass profiles together with the two available measurements of the mass of VCC 1287 (circles), obtaining a halo mass between $10.20 < \log_{10}(M_{\mathrm{halo}}/\mathrm{M}_\odot) < 10.80$, in agreement with estimates from Beasley et al. (2016). We also show DF 44 UDG (triangle) as in van Dokkum et al. (2016), who inferred a $\sim 8 \times 10^{11}$ M$_\odot$ halo mass for this galaxy: we show here that an $M_{\mathrm{halo}} = 10^{11.05}$ M$_\odot$ matches this observation, by plotting as dashed line the mass profile of a simulated UDG with a similar $M^\star$ as DF 44 and effective radius of 4.4 kpc (not shown in Fig. 1 due to magnitude cut), corroborating the finding that even the brightest UDGs are not Milky Way mass objects.

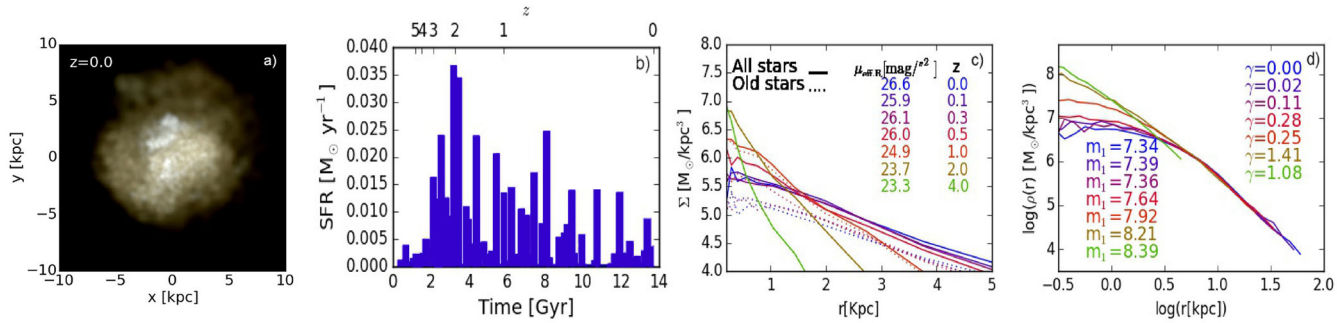


**Figure 3.** Formation of the UDG marked with a cross in Fig. 1. From left to right: (a) face-on multiband image of stars at $z = 0$, (b) SFH, (c) 3D spherically averaged stellar density profile colour coded by $z$ and (d) evolution of DM density profile. Panel (c): the contribution of all stars and old stars formed within the first 5 Gyr of the galaxy's life is indicated as solid and dashed line, respectively; the $\mu_e$ evolution is shown as well. Panel (d): the DM density inner slope measured within 1 and 2 per cent of the galaxy virial radius and the total enclosed mass at 1 kpc ($m_1 = \log_{10}(M_{<1\,kpc}/M_\odot)$) are indicated as a function of $z$.

Finally, the concentrations of simulated UDGs are typical of galaxies of their halo masses, excluding the possibility that UDGs form in haloes with $c$ systematically higher or lower than average.

### 3.2 UDGs: formation scenario

We analyse the properties of the UDG marked with a cross in Fig. 1 to show how such objects can form. In Fig. 3, we show (a) a visualization of the stellar distribution at $z = 0$ using a three-colour image based on *IVU* bands, (b) the star formation history (SFH) of the galaxy, (c) the evolution of the 3D stellar density as a function of redshift for all stars (solid lines) and old stars ($t_{form} < 5$ Gyr, dashed lines) and (d) the evolution of DM density, logarithmic inner slope $\gamma$ and total amount of mass $m_1 = \log_{10}(M_{<1kpc}/M_\odot)$ contained within 1 kpc of the galaxy as a function of redshift. The bursty SFH of the UDG can be appreciated in panel (b), including peaks in the last gigayear of its history, indicating recent episodes of star formation: this feature is also reflected in the blue off-centred overdensity visible in the colour image of panel (a), similar to DGSAT I UDG observed in Martínez-Delgado et al. (2016).

The formation scenario of UDGs is illustrated in panels (c) and (d): as the DM halo expands and forms a central core due to episodic and powerful gas outflows driven by star formation, the stellar distribution expands as well. In panel (c), the effective surface brightness is shown as a function of redshift: as $r_e$ increases, $\mu_e$ decreases bringing the dwarf on to the UDG regime. This galaxy became an ultra-diffuse one by $z = 1.5$. To confirm that $r_e$ increases due to expansion of the stellar distribution rather than by new episodes of star formation in the outer regions, we separate the contribution of all stars and old stars: we observe that even the oldest stellar population expands as a response to the core creation mechanism. A spatially extended stellar distribution, typical of UDGs, can therefore arise from internal feedback processes, which also give rise to a spherical rather than discy galaxy. An extensive study of UDGs morphologies will be presented in forthcoming work.

### 3.3 UDGs: gas content and star formation histories

We investigate what makes UDGs differ from more compact galaxies in the same stellar mass range. In Fig. 4, we show the SFH of six galaxies whose effective radii are the largest (right-hand column) and smallest (left-hand column) in their respective mass bin. Fig. 4 therefore includes both UDGs as well as more compact, regular dwarfs. From top to bottom, we pair galaxies with similar halo and stellar masses, quoting in each panel the $r_e$, $M_R$, $M^\star$, $M_{HI}$, extension

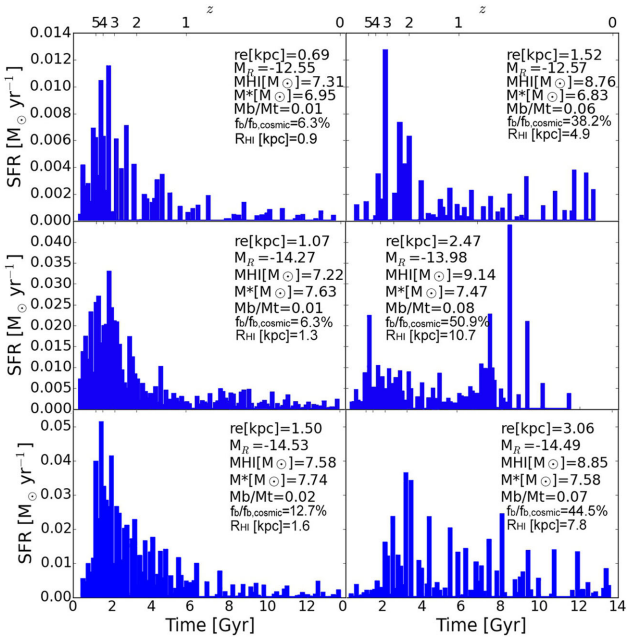


**Figure 4.** SFHs of galaxies with the largest (right-hand column) and smallest (left-hand column) effective radius in their mass bin. From top to bottom, each row shows galaxies with similar halo mass and magnitude, $\log_{10}(M_{halo}/M_\odot) \sim 10.20,10.45,10.50$ and $M_R \sim -12.5, -14.0, -14.5$. In each panel, $r_e$, $M_R$, $M_{HI}$, $M^\star$, $f_b$ and H I radius are indicated.

of H I gas ($R_{HI}$, as the radius at which the H I surface density reaches 1 $M_\odot$ pc$^{-2}$) and baryon fraction relative to the cosmic one, $f_{b,c}$.

The difference in properties between the most extreme UDGs (right-hand panels) and the less extreme, more compact dwarfs (left-hand panels) are striking. Galaxies with large $r_e$ also have a larger $M_{HI}$, baryon fraction and $R_{HI}$, and more prolonged and persistently bursty SFH, including a larger fraction of young stellar population, compared to galaxies with a smaller $r_e$. When most of star formation happens in the first ∼3–4 Gyr, feedback can eject significant amounts of gas from relatively shallow potential wells at early times (e.g. Dekel & Silk 1986), resulting in low baryon fractions by $z = 0$. Since gas is expelled at early stages, there is less gas for ongoing star formation and crucially there is less gas to be expelled from the inner regions when star formation occurs, being this the key aspect of the mechanism for core creation: the lower is the gas fraction at a given epoch, the less efficient is such mechanism. We verified that the dwarfs with lower $r_e$ have retained

at most 10 per cent of the initial gas mass between $z = 4$ and 1, while the largest $r_e$ UDGs have kept up to 50 per cent of the initial gas within the same period. The less expanded galaxies have a very low baryon fraction, $f_b/f_{b,c} \sim 6$–13 per cent by $z = 0$, and retain up to two order of magnitudes less H I gas than similar $M^\star$ galaxies with larger $r_e$; their DM inner slope is less shallow and correspondingly the distribution of H I is more compact, with $R_{\rm H\,I} \sim 0.9$–1.6 kpc.

Oppositely, galaxies with star bursts occurring after the rapid halo growth phase has finished are the ones which can keep their gas, which cannot escape the deeper potential well: they have enough gas available at all time to drive DM cores and a spatially extended stellar distribution, retaining about 50 per cent $f_{b,c}$ and up to $10^9$ $M_\odot$ in H I gas by $z = 0$. A similar dependence of core sizes with SFH has been found in Oñorbe et al. (2015) and Read et al. (2016) for lower mass objects than the ones studied here, with $M_{\rm halo} \sim 10^{7-10}$ $M_\odot$.

We conclude by summarizing the differences between regular dwarfs (such as the top-left galaxy in Fig. 4) and UDGs within a similar $M^\star$ range: non-UDGs have smaller effective radius, less gas mass and baryon fraction, steeper DM inner slope and a higher Sérsic index than UDGs, while their halo mass, colour, magnitude, spin parameter and concentration are indistinguishable from the ones of UDGs. This further validates the finding that the availability of gas is crucial to the formation mechanism of UDGs.

## 4 CONCLUSIONS

We showed that cosmological simulations of isolated galaxies from the NIHAO project, which include feedback from SNe and massive stars, reproduce a population of UDGs with stellar mass, magnitude, colour, Sérsic index, effective radius and surface brightness in agreement with observations. Internal processes, rather than environmental ones, are at the base of the formation scenario of UDGs. Feedback-driven gas outflows give rise to a spatially extended stellar component, while simultaneously expanding the DM halo, leading to the emergence of LSB dwarf galaxies, or UDGs, with $M^\star \sim 10^{7-9}$ $M_\odot$ and $r_e \sim 1$–3 kpc. A key aspect is the availability of gas which is driven away from central regions during bursts of star formation, causing rapid oscillations of the potential: galaxies which expel most of their gas at early times are less efficient at causing expansion than galaxies of similar $M^\star$ that retain more gas for later times. Our findings imply that UDGs

(i) are dwarf galaxies, with $10^{10} \lesssim M_{\rm halo}/M_\odot \lesssim 10^{11}$, in agreement with mass estimates from Beasley et al. (2016), Beasley & Trujillo (2016) and Peng & Lim (2016), and with our revised mass estimate of the van Dokkum et al. (2016) DF 44 UDG: they naturally extend the population of LSB galaxies to the dwarf regime;

(ii) are not exclusively associated with a cluster environment: they are expected to be found in the field as well;

(iii) are not all red and quenched: we found simulated UDGs with $B-R < 0.7$ and recent off-centred star formation, as well as UDGs with $B-R > 0.7$ which only stopped forming stars in the past 2 Gyr;

(iv) have typical distributions of halo spin and concentration, an average Sérsic index of less than 1 and DM cores;

(v) if isolated, have significant H I gas mass, $M_{\rm H\,I} \sim 10^{7-9}$ $M_\odot$: at a similar stellar mass, the larger the effective radius, the higher is the baryon fraction retained within the virial radius and the larger is the amount and extent of H I gas, with $R_{\rm H\,I}$ up to ∼10.7 kpc; moreover, the larger $r_e$, the higher is the fraction of young stellar population expected in isolated UDGs.

The first three points of the list are in common with the model of Amorisco & Loeb (2016) although, unlike our scenario, those authors appealed to high spin haloes in order to form UDGs.

Given their predicted $M_{\rm H\,I}$, some UDGs should be seen, or have already been seen, by the H I Alfalfa survey (Giovanelli et al. 2005; Haynes et al. 2011). Indeed, some *dark galaxies* in Alfalfa, those without a clear optical counterpart, have only recently been identified with LSB objects (Cannon et al. 2015) and have H I mass $7.4 < \log(M_{\rm H\,I}/M_\odot) < 9.5$. Deep optical imaging (Janowiecki et al. 2015) shows that the system H I1232+20 has magnitude, H I mass, surface brightness, colours and remarkably a large $R_{\rm H\,I}$ (5.1–11.2 kpc) in agreement with our most expanded UDGs. The fraction of *dark galaxies* over the total number of detected H I sources, within a completeness radius of 20 Mpc and having the expected $M_{\rm H\,I}$ mass of UDGs, is as high as 8.5 per cent in the Alfalfa $\alpha.70$ catalogue: some of them may be UDGs, and future dedicated observations can help verify our claim. Finally, in the SPARC sample of local H I-rich galaxies (Lelli, McGaugh & Schombert 2016), 70 per cent of the galaxies with $10^7 < M^\star/M_\odot < 10^{8.5}$ have $r_e > 1$ kpc, whilst 20 per cent have $r_e > 2$ kpc, giving surface brightnesses in the realm of UDGs, and showing that such sizes are not rare amongst dwarfs after all.

We proposed a scenario in which UDGs form naturally by outflow episodes in haloes of $M_{\rm halo} \sim 10^{10-11}$ $M_\odot$, in the same mass range where feedback-induced expansion is expected to be most efficient at creating a cored distribution of DM and stars (e.g. Di Cintio et al. 2014a; Dutton et al. 2016; Tollet et al. 2016): the existence of a preferential halo mass for UDGs therefore fits within our theoretical understanding of how stellar feedback impacts the DM and stellar distribution in galaxies. This picture agrees with models in which the effect of repeated outflows accumulates during cosmic time (e.g. Read & Gilmore 2005; Pontzen & Governato 2012; Dutton et al. 2016): we demonstrate here for the first time that it is the gas availability which drives both the SFH and the amount of expansion of DM and stars, with higher gas fractions more efficiently expanding both the stellar and DM component, leading to the emergence of LSB, gas-rich, H I extended UDGs.

Larger diffuse galaxies, with $r_e$ up to 7–8 kpc, exist as well in the NIHAO simulations, with $M^\star$ higher than the presently observed UDGs: they can be classified as regular LSBs and will be the subject of a future paper (Di Cintio, in preparation).

## ACKNOWLEDGEMENTS

The authors kindly thank M. Yagi, J. Koda, I. Trujillo, J. Roman, M. Beasley, E. Papastergis, M. Haynes, F. Lelli and N. Amorisco for sharing their data and for fruitful discussions. Computational resources were provided by the High Performance Computing at NYUAD, the THEO cluster at MPIA and the HYDRA clusters at Rechenzentrum in Garching. ADC thanks the Carlsberg foundation. CBB thanks MINECO/FEDER grant AYA2015-63810-P. AD is supported by grants ISF124/12, BSF 2014-273.

## REFERENCES

Amorisco N. C., Loeb A., 2016, MNRAS, 459, L51
Beasley M. A., Trujillo I., 2016, ApJ, 830, 23
Beasley M. A., Romanowsky A. J., Pota V., Navarro I. M., Martinez Delgado D., Neyer F., Deich A. L., 2016, ApJ, 819, L20
Brook C. B., Stinson G., Gibson B. K., Wadsley J., Quinn T., 2012, MNRAS, 424, 1275

Bullock J. S., Dekel A., Kolatt T. S., Kravtsov A. V., Klypin A. A., Porciani C., Primack J. R., 2001, ApJ, 555, 240
Cannon J. M. et al., 2015, AJ, 149, 72
Chan T. K., Kereš D., Oñorbe J., Hopkins P. F., Muratov A. L., Faucher-Giguère C.-A., Quataert E., 2015, MNRAS, 454, 2981
Dekel A., Silk J., 1986, ApJ, 303, 39
Di Cintio A., Brook C. B., Macciò A. V., Stinson G. S., Knebe A., Dutton A. A., Wadsley J., 2014a, MNRAS, 437, 415
Di Cintio A., Brook C. B., Dutton A. A., Macciò A. V., Stinson G. S., Knebe A., 2014b, MNRAS, 441, 2986
Dutton A. A. et al., 2016, MNRAS, 461, 2658
El-Badry K., Wetzel A., Geha M., Hopkins P. F., Kereš D., Chan T. K., Faucher-Giguère C.-A., 2016, ApJ, 820, 131
Giovanelli R. et al., 2005, AJ, 130, 2598
Governato F. et al., 2010, Nature, 463, 203
Gutcke T. A., Stinson G. S., Macciò A. V., Wang L., Dutton A. A., 2016, MNRAS, preprint (arXiv:1602.06956)
Haynes M. P. et al., 2011, AJ, 142, 170
Impey C., Bothun G., 1997, ARA&A, 35, 267
Janowiecki S. et al., 2015, ApJ, 801, 96
Katz H., Lelli F., McGaugh S. S., Di Cintio A., Brook C. B., Schombert J. M., 2016, MNRAS, preprint (arXiv:1605.05971)
Keller B. W., Wadsley J., Benincasa S. M., Couchman H. M. P., 2014, MNRAS, 442, 3013
Knollmann S. R., Knebe A., 2009, ApJS, 182, 608
Koda J., Yagi M., Yamanoi H., Komiyama Y., 2015, ApJ, 807, L2
Lelli F., McGaugh S. S., Schombert J. M., 2016, AJ, preprint (arXiv:1606.09251)
Macciò A. V., Dutton A. A., van den Bosch F. C., 2008, MNRAS, 391, 1940
Martínez-Delgado D. et al., 2016, AJ, 151, 96
Mashchenko S., Wadsley J., Couchman H. M. P., 2008, Science, 319, 174
McGaugh S. S., Schombert J. M., Bothun G. D., 1995, AJ, 109, 2019
Mihos J. C. et al., 2015, ApJ, 809, L21
Muñoz R. P. et al., 2015, ApJ, 813, L15
Obreja A., Stinson G. S., Dutton A. A., Macciò A. V., Wang L., Kang X., 2016, MNRAS, 459, 467
Oñorbe J., Boylan-Kolchin M., Bullock J. S., Hopkins P. F., Kereš D., Faucher-Giguère C.-A., Quataert E., Murray N., 2015, MNRAS, 454, 2092
Peng E. W., Lim S., 2016, ApJ, 822, L31
Pontzen A., Governato F., 2012, MNRAS, 421, 3464
Pontzen A., Roškar R., Stinson G., Woods R., 2013, Astrophysics Source Code Library, record ascl:1305.002
Read J. I., Gilmore G., 2005, MNRAS, 356, 107
Read J. I., Agertz O., Collins M. L. M., 2016, MNRAS, 459, 2573
Roman J., Trujillo I., 2016, preprint (arXiv:1603.03494)
Sandage A., Binggeli B., 1984, AJ, 89, 919
Schombert J., Maciel T., McGaugh S., 2011, Adv. Astron., 2011, 143698
Sersic J. L., 1968, Atlas de Galaxias Australes. Observatorio Astronomico, Cordoba
Shen S., Wadsley J., Stinson G., 2010, MNRAS, 407, 1581
Stinson G., Seth A., Katz N., Wadsley J., Governato F., Quinn T., 2006, MNRAS, 373, 1074
Stinson G. S., Brook C., Macciò A. V., Wadsley J., Quinn T. R., Couchman H. M. P., 2013, MNRAS, 428, 129
Teyssier R., Pontzen A., Dubois Y., Read J. I., 2013, MNRAS, 429, 3068
Tollet E. et al., 2016, MNRAS, 456, 3542
van der Burg R. F. J., Muzzin A., Hoekstra H., 2016, A&A, 590, A20
van Dokkum P. G., Abraham R., Merritt A., Zhang J., Geha M., Conroy C., 2015a, ApJ, 798, L45
van Dokkum P. G. et al., 2015b, ApJ, 804, L26
van Dokkum P. et al., 2016, ApJ, 828, L6
Wadsley J. W., Stadel J., Quinn T., 2004, New Astron., 9, 137
Wadsley J. W., Veeravalli G., Couchman H. M. P., 2008, MNRAS, 387, 427
Wang L., Dutton A. A., Stinson G. S., Macciò A. V., Penzo C., Kang X., Keller B. W., Wadsley J., 2015, MNRAS, 454, 83
Yagi M., Koda J., Komiyama Y., Yamanoi H., 2016, ApJS, 225, 11
Yoshida M., Yagi M., Ohyama Y., Komiyama Y., Kashikawa N., Tanaka H., Okamura S., 2016, ApJ, 820, 48
Yozin C., Bekki K., 2015, MNRAS, 452, 937

This paper has been typeset from a TEX/LATEX file prepared by the author.